Template Effects in SN2 Displacements for the Preparation of Pseudopeptidic Macrocycles

ARTICLE *in* CHEMISTRY - A EUROPEAN JOURNAL · FEBRUARY 2012

Impact Factor: 5.73 · DOI: 10.1002/chem.201101416 · Source: PubMed

3 AUTHORS:

Vicente Martí-Centelles
The University of Edinburgh
33 PUBLICATIONS **82** CITATIONS
SEE PROFILE

Maria Isabel Burguete
Universitat Jaume I
223 PUBLICATIONS **3,603** CITATIONS
SEE PROFILE

Santiago V. Luis Lafuente
Universitat Jaume I
336 PUBLICATIONS **5,376** CITATIONS
SEE PROFILE

DOI: 10.1002/chem.201101416

Template Effects in S_N2 Displacements for the Preparation of Pseudopeptidic Macrocycles

Vicente Martí-Centelles, M. Isabel Burguete, and Santiago V. Luis*[a]

Abstract: Macrocyclisation reactions of C_2-symmetric pseudopeptides containing central pyridine-derived spacers are affected by the presence of different anions. The selection of the proper anion gives excellent results for the preparation of the corresponding macrocyclic structures. Kinetic studies show that the presence of those anions enhances both the yield and the rate of the reaction. Computational studies at the B3LYP/6-31G* level have allowed us to rationalise the experimental results. The obtained transition states (TSs) show that the interaction between the anion and the open-chain pseudopeptidic chain has a stabilising effect. The anion stabilises the two TSs involved: the first one, which involves the formation of the initial bond between the two subunits and leads to an open-chain intermediate, and the second one, which precedes the formation of the cyclic structure. The optimum anion (Br^- when the central spacer is derived from 2,6-bis(aminomethyl)pyridine, is able to act as a template, in that it forces the two ends of the open-chain intermediate to approach each other by forming hydrogen bonds with the two amino acid subunits present in the intermediate. This stabilises the second TS to a greater extent than the first one, and thus, favours macrocyclisation over the competing oligomerisation reactions. The computational calculations also allowed us to predict the outcome of new experiments. Accordingly, the synthesis of the pseudopeptidic macrocycle derived from 2,6-diaminopyridine was not successful under the optimised conditions previously used. Nevertheless, calculations predicted that in this case Cl^- should be more efficient than Br^-, and this was subsequently experimentally confirmed. Interestingly, the presence of different substituents on the constituent amino acids seems to play a minor role in the overall process.

Keywords: anions · macrocycles · pseudopeptides · supramolecular chemistry · template effects

Introduction

Macrocyclic structures play an important role in nature. The generation of a macrocyclic structure represents a simple protocol that involves the preorganisation of a significant number of functional groups with the appropriate disposition at the proper distance.[1] Many antibiotics, and in particular those that are able to act by inactivation of bacterial ribosomes, contain macrolide structures.[2] In this regard, cyclopeptides have been shown to take part in important biological functions,[3] with the natural antibiotic vancomycin being one of the earliest known examples of this kind of compounds.[4] Many other important cyclopeptidic structures include the hormone oxytocine,[5] the related neuropeptide vasopressin,[5b] the antibiotics cyclosporine[6] and tyrocidine A,[7] and some apoptosis-inducing cyclopeptides with antitumour properties.[8] Their cyclic structure enhances their activity,[9] their physicochemical stability and provides a mechanism for resistance towards proteases.[3,10] Thus, much attention has been recently drawn to the preparation of macrocyclic structures containing amino acids.[1,11] In most cases, the preparation of those multifunctional molecules is limited by the macrocyclisation step. This step needs to efficiently compete with intermolecular dimerisation and oligomerisation processes, and can be kinetically or thermodynamically controlled, depending on the irreversible or reversible nature of the cyclisation reaction.[12] Entropic and enthalpic factors contribute to achieve an adequate conformational arrangement, leading to the desired regio- and stereochemistry.[13] For this purpose, complex synthetic routes need to be devised. These require specifically designed protection and deprotection steps, high-dilution techniques or specific protocols, such as ring-closing metatheses,[14] Ugi processes,[15] click chemistry processes[16] or chemoenzymatic approaches.[17,18] Competing oligomerisation processes are, in general, favoured by entropic factors. Thus, in successful macrocyclisations, open-chain precursors are preorganised in a folded conformation, in which the two reacting sites are in proximity.[19] This arrangement, with the appropriate orientation, provides an unencumbered trajectory of attack and accelerates the intramolecular process, so that it becomes competitive with the intermolecular process.[20] In recent years, we have been working on the preparation of pseudopeptidic macrocycles, such as **1** and **2**, which can be

[a] V. Martí-Centelles, Prof. Dr. M. I. Burguete, Prof. Dr. S. V. Luis
Departament de Química Inorgànica i Orgànica
Universitat Jaume I 12071 Castelló (Spain)
Fax: (+34) 964-728-214
E-mail: luiss@qio.uji.es

Supporting information for this article is available on the WWW under http://dx.doi.org/10.1002/chem.201101416.

prepared from a common intermediate **3** (Figure 1). For smaller [1+1] macrocycles **1**, the successful reaction of **3** with a bis(bromomethyl)arene, is based on the preorganisation of the precursor **3**, and that of the corresponding inter-

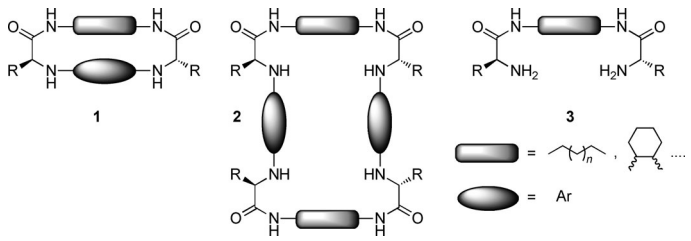

Figure 1. General representation of the macrocyclic and open-chain pseudopeptidic structures.

mediate afterwards. Derivatives of α,ω-diamino alkanes, adopt a U-turn folded conformation because of intramolecular interactions and solvophobic forces.[21] The synthesis of larger [2+2] macrocycles **2** is accomplished by reaction of **3** with aromatic dialdehydes. When a chiral 1,2-cyclohexane diamine is used as the spacer, proper preorganisation can be achieved based on configurational traits and the match/mismatch between the configuration of the diamine and that of the amino acid determine the success of the macrocyclisation.[22,23] When flexible spacers ($-(CH_2)_n-$) are used, though, the use of an anionic template is imperative.[24] This is an attractive strategy because one could select the specific template best-suited for each macrocyclisation reaction.[24,25,26] Nevertheless, the use of thermodynamic templates is only possible for reversible reactions (i.e., the imine formation in the preparation of **2**). Thus, this approach is unsuitable for macrocycle syntheses that involve an irreversible cyclisation reaction (e.g., S_N2 reactions). Herein, we show how the use of anionic kinetic templates, which preferentially stabilise the transition state (TS) of the cyclisation step instead of that of the oligomerisation process (increasing in $k_{cyclisation}/k_{oligomerisation}$), is a useful tool for optimising macrocyclisation. A thorough computational study has been carried out to understand this process and the results obtained nicely agree with experimental data. Moreover, the use of computational techniques has allowed us to optimise template characteristics and determine the conditions required for the synthesis of a very strained macrocycle.

Results and Discussion

Most of our previous work with pseudopeptidic compounds **1–3** has been carried out using the general structure **3**, which was derived from 1,2-cyclohexane diamines or α,ω-aliphatic diamines. The conformational freedom provided by the flexible $-(CH_2)_n-$ spacer and its easy sequential variation were useful for gaining insights into the role of the different structural elements on the properties of the resulting compounds. This was especially important when self-assembly processes in solution or in the solid state were examined.[27–29] On the other hand, our initial studies on the catalytic applications of those simple pseudopeptides, as well as those of Dangel et al.,[30] suggested that the substitution of an aliphatic spacer by an aromatic one can be an interesting structural modification (Scheme 1).[31] Thus, taking into ac-

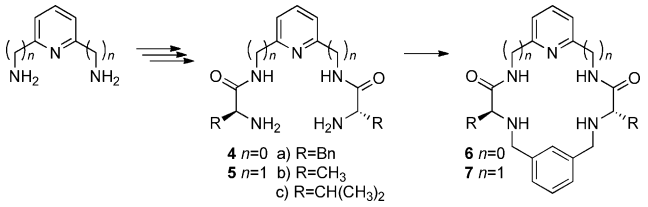

Scheme 1. Synthetic route for the preparation of pyridine-containing pseudopeptidic macrocycles. General conditions for the macrocyclisation reaction: acetonitrile as the solvent, the corresponding base (10 equiv), TBAX (TBA = tetrabutylammonium, X = anion; 0.5 equiv) and 1,3-bis-(bromomethyl)benzene (1 equiv). Bn = benzyl.

count previous studies into the use of different pyridine-containing receptors (particularly polyazapyridinophanes) in molecular recognition processes,[32,33] we selected structures **6** and **7** as our synthetic targets. For this purpose, the corresponding open-chain pseudopeptides **4** and **5** were easily prepared from 2,6-diaminopyridine and 2,6-bis(aminomethyl)pyridine. Compound **5** was prepared by reaction of the diamine with the *N*-hydroxysuccinimide ester of the proper amino acid, under the conditions previously reported for the preparation of open-chain pseudopeptides containing aliphatic spacers (**3**).[21] In the case of 2,6-diaminopyridine, its low reactivity required the activation of the corresponding amino acid through the formation of a mixed anhydride of ethyl chloroformate.[34] The macrocyclisation was then investigated under conditions similar to those used for the synthesis of **1** from **3**. Those conditions involved the use of acetonitrile at reflux as the solvent, anhydrous K_2CO_3 as the base and tetrabutylammonium bromide (TBABr; 0.5 equiv) as the phase-transfer reagent. The use of TBABr (or other TBAX salts) was required because most of the K_2CO_3 was not dissolved. After 24 h, the expected product **7a** ($n=1$, $R=CH_2Ph$) was isolated in 87% yield after the usual workup. The formation of **6a** ($n=0$, $R=CH_2Ph$) could be detected by MS, but the yield was so low that it could not be isolated and purified. Careful analysis of the MS spectra of the crude reaction mixture confirmed that the cyclisation was not very efficient and that polymerisation/oligomerisation processes were prevalent. Thus, the MS spectra revealed that along with the expected signal at m/z 585 [M+H] for the macrocyclic compound **6a**, important signals corresponding to the open-chain intermediate **8a** (at m/z 586–588 [M'+H]), and the successive open-chain oligomerisation products **10a**, **12a** and **14a** were also present. The identity of the structures corresponding to those peaks was unequivocally identified by high-resolution (HR) MS and through the isotopic pattern analysis of the corresponding clusters

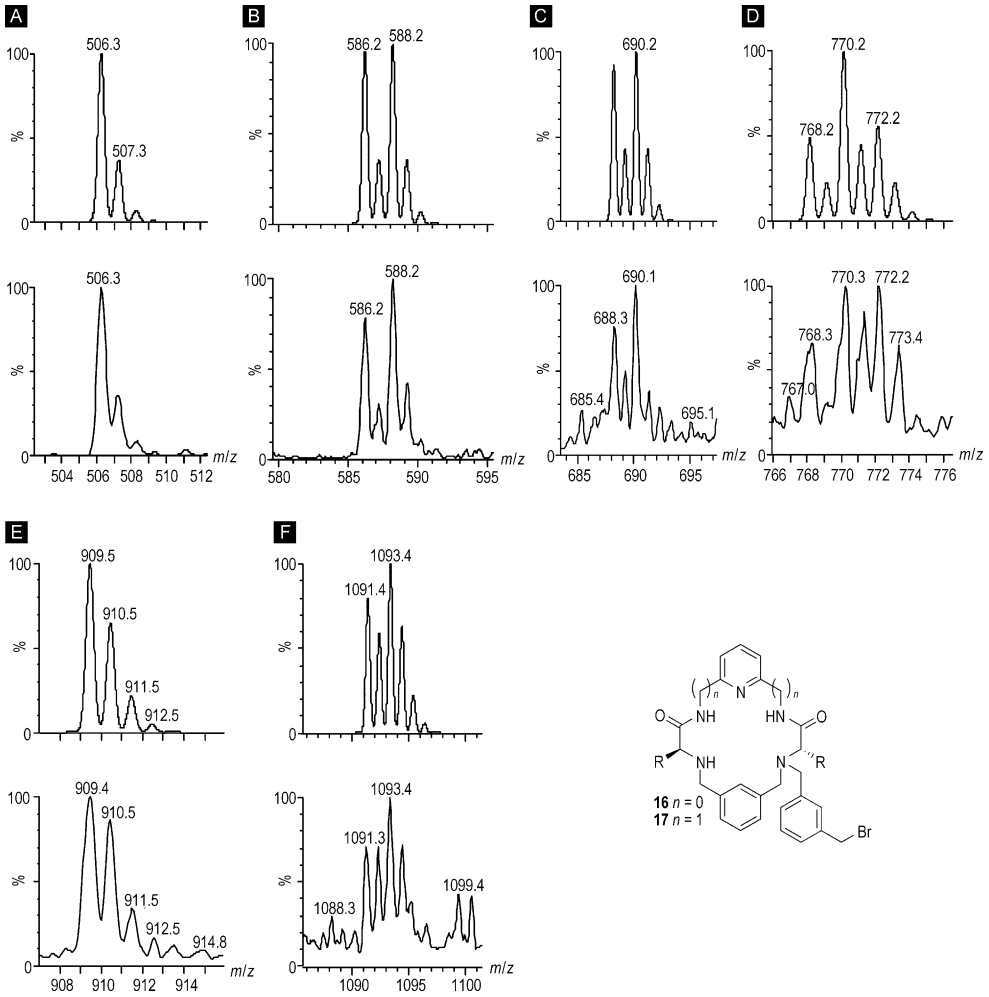

Figure 2. Experimental (bottom) and theoretical (top) isotopic patterns corresponding to the peaks for the different open-chain compounds obtained in the attempted preparation of **6a**: A) **6a**, B) **8a**, C) **16a**, D) **14a**, E) **12a**, F) **10a**.

(Figure 2). HRMS analysis also showed the presence of the N-alkylated macrocycle **16a**. This again confirmed that the N-alkylation processes, not involving the formation of the ring, efficiently compete with macrocyclisation (Scheme 2). As for the synthesis of **7**, we varied reaction conditions to achieve optimal yields (Table 1). Interestingly, in the absence of a base (entry 7, Table 1) the maximum attainable yield was 59%. This suggested that the molecules of **5** acted as the base and neutralised the ammonium salts formed after each N-alkylation. In good agreement with this, the precipitation of the trihydrobromide salt of the bis-amino amide was observed with the progress of the reaction. A second observation was that the best yields were associated with the presence of TBABr (entries 1 and 4, Table 1) and/or K_2CO_3 (entry 1, Table 1). The presence of Cl^- or F^- (entries 5 and 6, Table 1) produced a significant decrease in the yield. This is of particular relevance for the fluoride anion, for which a large number of side products, most likely associated with its behaviour as a strong base, were obtained. Subsequently, we carried out a thorough kinetic analysis of the macrocyclisation processes. For this, we developed an HPLC protocol that allowed the separation and identification of the main components of the reaction mixtures. Of particular relevance for the kinetic analysis was the identification of **5**, 1,3-bis(bromomethyl)benzene and **7** (Scheme 2). The open-chain intermediate **9** and some of the oligomeric side products were also separated and identified (Figure 3). The identity of each HPLC signal was assigned by comparison, when possible, with authentic samples and by a complete HPLC–HRMS analysis of the corresponding mixtures. Alternatively, the corresponding kinetics could also be followed by NMR spectroscopy (amide, benzylic and methine (stereogenic centre) protons were monitored (Figure 4)). Evidently, the different reaction conditions not only affected yields, but also, very significantly, the kinetics of the process (Figure 5). The data for F^- (entry 6 in Table 1) have not been included in Figure 5 because the presence of a large number of side products does not permit obtaining accurate kinetic curves. For the sake of comparison, Figure 6 shows the kinetic curves obtained at 25°C under the conditions shown in Table 1, entry 4, by using NMR spectroscopy. Higher concentrations are required to carry out the NMR

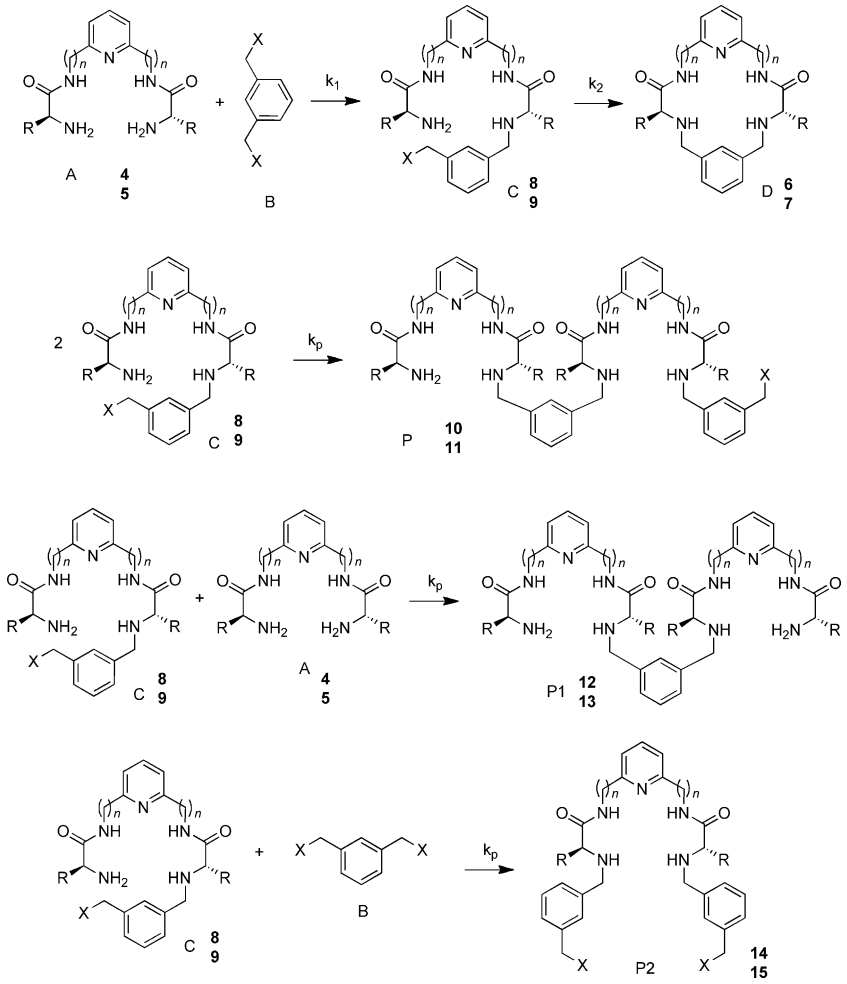

Scheme 2. Overall reaction sequence including significant side reactions.

Table 1. Results obtained in the synthesis of **7** under different macrocyclisation conditions.[a]

Entry	Solvent	Base	TBAX[b]	Yield [%][c]
1	CH_3CN	K_2CO_3[d]	Br	93
2	CH_3CN	DIPEA[e]	–	82
3	CH_3CN	DIPEA[e]	AcO	69
4	CH_3CN	DIPEA[e]	Br	96
5	CH_3CN	DIPEA[e]	Cl	81
6	CH_3CN	DIPEA[e]	F	30[f]
7	CH_3CN	–	–	58[g]

[a] All reactions were heated to reflux. [b] 0.5 equiv. [c] Determined by HPLC from the crude reaction mixture. [d] Excess of solid anhydrous salt. [e] DIPEA = diisopropylethylamine; 10 equiv of base were added. [f] A very complex mixture was obtained. [g] Under those conditions the triprotonated bis-aminoamide precipitated.

spectroscopy experiments because of an increased contribution from oligomerization processes. As seen in Figure 5, the different reaction conditions assayed do not only affect the yield of the reaction, but also, very significantly, the kinetics of the process. Optimum results (in terms of kinetics and final yields) were obtained with DIPEA as the base in the presence of TBABr. This was attributed to the presence of Br^- at the beginning of the reaction and the fact that Br^- is continually produced by the alkylating agent. For the initial conditions (entry 1, Table 1) the potential exchange between TBABr and $(TBA)_2CO_3$ accounted for the slower kinetics observed at the beginning of the reaction. As the process progressed, the amount of Br^- increased and the kinetics of the reaction gradually resembled those of processes in which Br^- is the only anion present. Similar kinetics were observable for the conditions given in Table 1, entries 2, 3 and 5. The consumption of **5a** in two different processes, N-alkylation/macrocyclisation, and its role as a base, led to a rapid rate decrease when no base was added (entry 7, Table 1). No significant kinetic effect was ascribed to Cl^-. Thus, the Br^- anion had a clear catalytic effect on the macrocyclisation reaction, and potentially a role as a kinetic anion template, stabilising the TS leading to the macrocycle.

Computational studies were then carried out to shed light on the issue. For this purpose, the different stationary points for the process under consideration were fully optimised at the B3LYP/6-31G* level of theory with the Gaussian 03 program.[35] For all cases, the optimised structures were confirmed as true minima by an

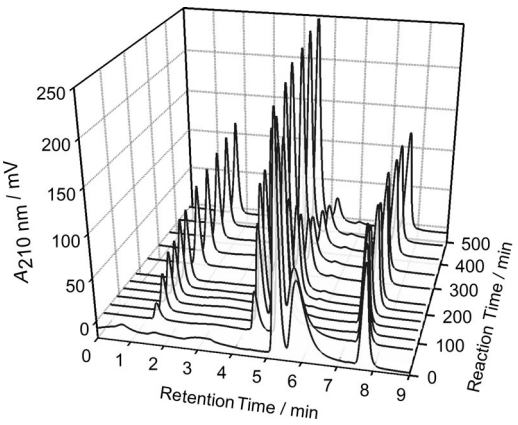

Figure 3. HPLC chromatograms obtained from the reaction mixture under the conditions considered in entry 2 of Table 1. Retention times: **7a** 4.61 min, 1,3-bis(bromomethyl)benzene 5.29 min, **5a** 6.15 min, mesitylene (internal standard) 7.64 min.

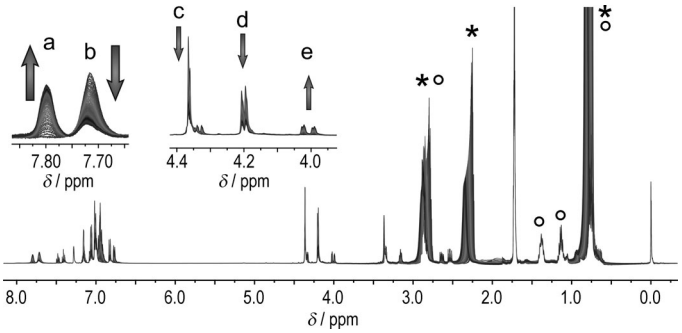

Figure 4. Kinetic analysis of the macrocyclisation process for the preparation of **7a** under the conditions reported in entry 4 of Table 1 (25 °C). a) $\delta = 7.80$ ppm, amide NH of **7a**. b) $\delta = 7.71$ ppm, amide NH of **5a**. c) $\delta = 4.37$ ppm. CH_2 of 1,3-bis(bromomethyl)benzene. d) $\delta = 4.20$ ppm, CH_2–pyridine of **5a**. e) $\delta = 4.00$ ppm, CH_2–pyridine of **7a**. Signals marked with an asterisk correspond to DIPEA; signals marked with an open circle correspond to TBA. Tetrakis(trimethylsilyl)silane was used as the internal standard at $\delta = 0$ ppm.

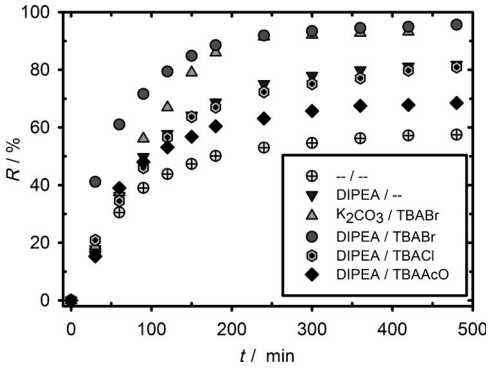

Figure 5. Kinetic curves obtained by HPLC for the formation of **7a** under the different reaction conditions reported in Table 1. Data for F^- (entry 6, Table 1) were omitted because the large number of side products prevented accurate kinetic analysis.

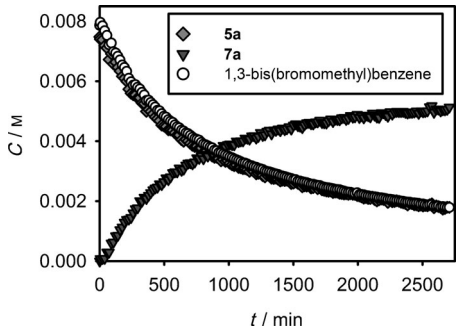

Figure 6. Kinetic curves obtained by NMR spectroscopy at 25 °C for the formation of **7a** under the experimental conditions described in Table 1, entry 4.

analysis of normal vibration modes. The alanine derivatives **5b**, **7b** and **9b** were selected as models for the open-chain precursor, the macrocyclic system and the intermediate, respectively. This significantly reduced the number of atoms relative to **5a**, **7a**, and **9a**, and, accordingly, the calculation time. Moreover, this eliminated the need to perform conformational analyses associated with the side chain. For proper analysis of the role of different anions, we compared the relative activation energies of different reaction steps.

The two major steps in the process are shown in Schemes 3 and 4. The first step involved the formation of intermediate **9b**, which, subsequently, cyclised in the second step. An efficient anionic catalyst should, thus, selectively reduce the activation energy of the cyclisation step more than it reduces the activation energy of the first step. In this approach, we assumed that the energy barriers for the different oligomerisation steps competing with the cyclisation were very similar to that of the first step because they involved a similar process and the presence of a given anion produced an equal effect on them. The structures of reactants, complexes of interaction of reactants (RIC), TSs, complexes of interaction of products (PIC), and products were optimised to obtain the corresponding reaction profiles. Initially, we carried out a potential energy surface (PES) calculation at the ONIOM (B3LYP/6-31G*:PM3) level of theory, which allowed us to find the approximate TS geometry and that of the other stationary points (Figure 7). The full optimisation of all the stationary points obtained from the PES analysis was then carried out at the B3LYP/6-31G* level (Figures 8 and 9). It was found that the anion was always efficiently bound in either of the TSs for the two reaction steps. All of the anions seemed to act as templates in the TS of the macrocyclisation step because supramolecular interactions between the anion and the two amide fragments in **8b** enforced a closed conformation, which brought the reactive sites in close proximity.[36] We then calculated the energy

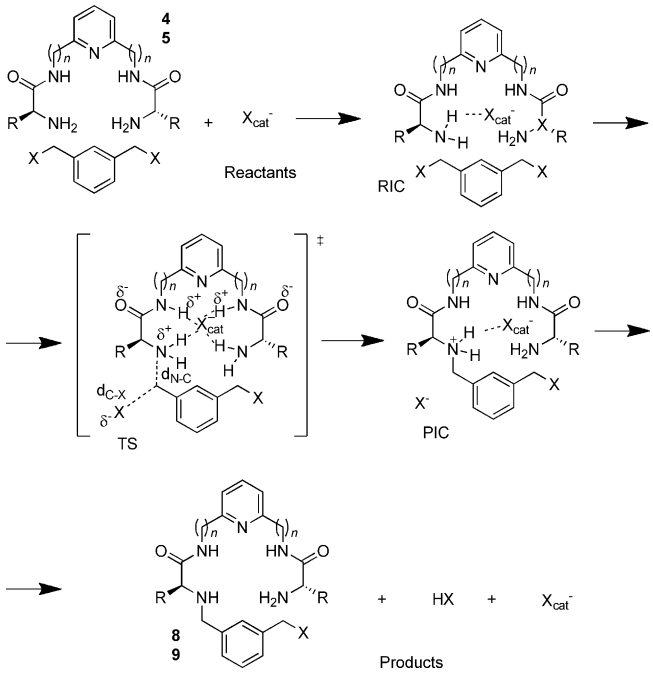

Scheme 3. Representation of the first step of the macrocyclisation process that leads to the corresponding open-chain intermediates **8** and **9** in the presence of X^-.

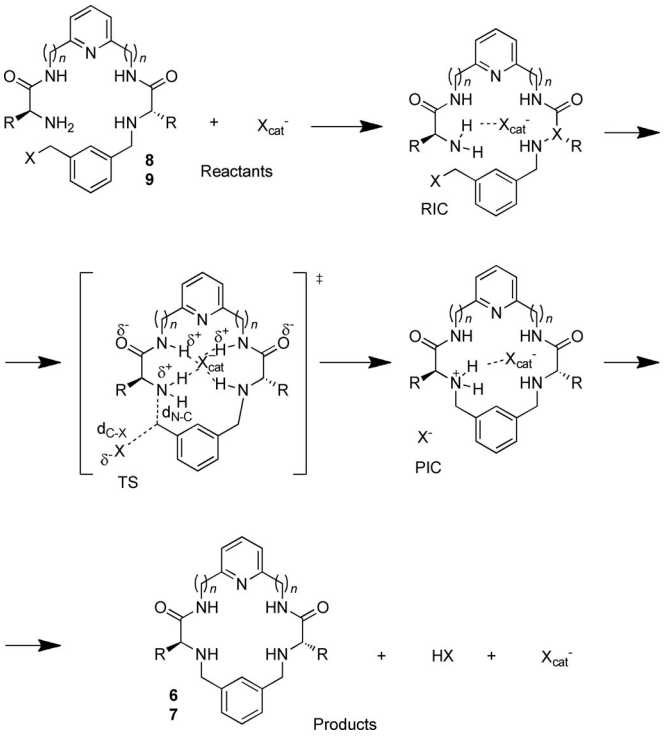

Scheme 4. Representation of the second step of the macrocyclisation process involving the formation of the macroring from the corresponding open-chain intermediates **8** and **9** in the presence of X^-.

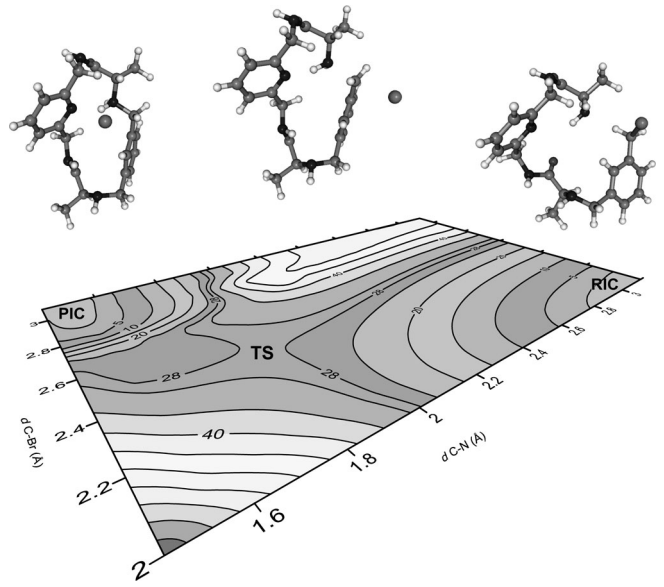

Figure 7. PES of the macrocyclisation reaction at the ONIOM (B3LYP/6-31G*:PM3 level of theory, in the absence of any additional anion, for the transformation of **9b** into **7b**.

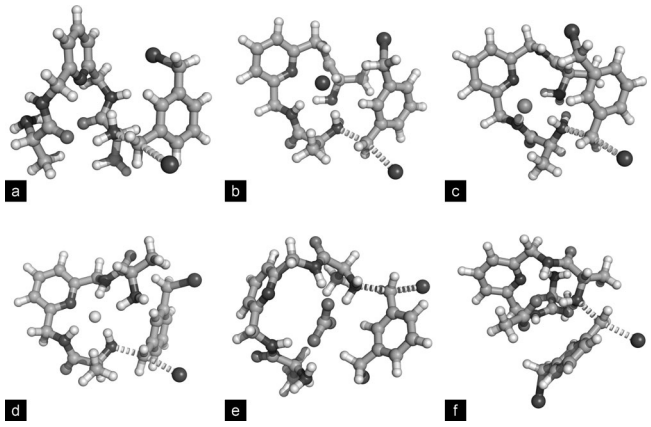

Figure 8. Fully optimised structures (B3LYP/6-31G*) for the TSs for the first reaction step for the preparation of **7b** in the presence of different anions: a) none, b) Br^-, c) Cl^-, d) F^-, e) CO_3^{2-} and f) AcO^-.

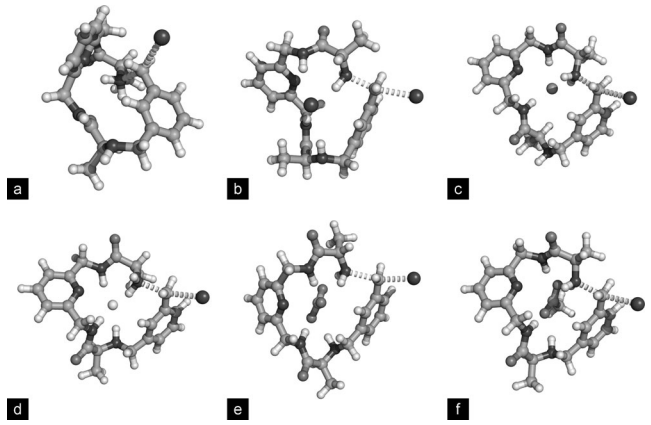

Figure 9. Fully optimised structures (B3LYP/6-31G*) for the TSs for the second reaction step for the preparation of **7b** in the presence of different anions: a) none, b) Br^-, c) Cl^-, d) F^-, e) CO_3^{2-} and f) AcO^-.

Table 2. Gibbs energy barriers [kcal mol^{-1}] for the first step of the reaction from **5b**.

	No cat.	CO_3^{2-}	Br^-	Cl^-	F^-	Acetate
reactants–RIC	3.07	−139.86	−29.06	−21.40	−98.28	−27.38
RIC–TS	25.80	13.18	20.93	17.93	16.25	17.07
TS–PIC	−17.79	−55.18	−24.17	−27.14	−26.53	−25.76
PIC–products	−2.09	190.85	41.30	39.60	117.55	45.06

Table 3. Gibbs energy barriers [kcal mol^{-1}] for the second step of the reaction (cyclisation of **9b**).

	No cat.	CO_3^{2-}	Br^-	Cl^-	F^-	Acetate
reactants–RIC	0.00	−137.67	−41.15	−36.42	−107.30	−41.22
RIC–TS	31.76	12.60	18.42	19.77	20.23	20.77
TS–PIC	−40.04	−51.39	−27.93	−18.49	−21.14	−21.14
PIC–products	0.03	168.21	42.41	26.90	99.96	33.34

barriers from the corresponding energy values of the optimised structures of the different stationary points (Tables 2 and 3). In the associated energy profiles in Figures 10 and 11, it can be seen that all anions had a catalytic effect on both reaction steps, reducing the values of the corresponding RIC–TS free-energy barriers. In all cases, the catalytic effect on the macrocyclisation step was more pronounced than on the first step. This agreed with the template effect observed for the structures of the different TSs. In the first step, the most favourable effect was calculated for the

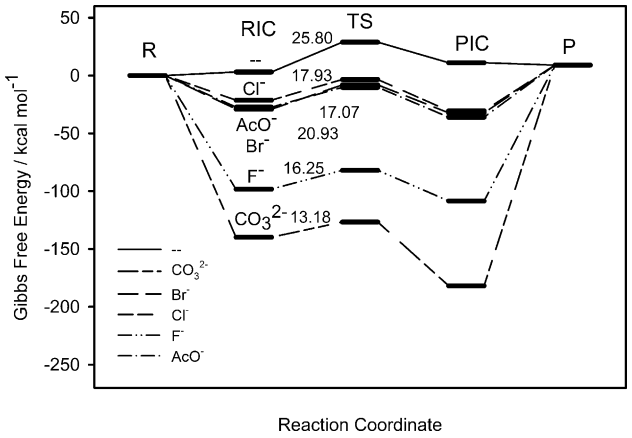

Figure 10. Calculated energy profile for the first step of the reaction from **5b**. The values for the RIC–TS barrier for each profile have been included [kcal mol^{-1}].

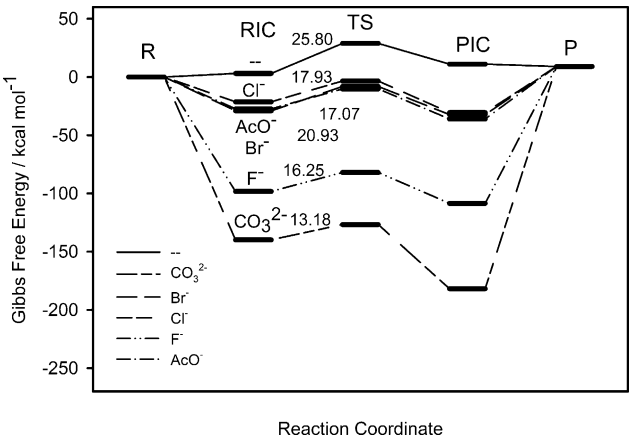

Figure 11. Calculated energy profile for the second step of the reaction (cyclisation of **9b**). The values for the RIC–TS barrier for each profile have been included [kcal mol^{-1}].

CO_3^{2-} anion, which decreased the RIC–TS barrier by 12.62 kcal mol^{-1} relative to that obtained for the process in the absence of anions. On the contrary, Br^- was the anion with the smallest effect for this step, reducing the corresponding energy barrier by just 4.87 kcal mol^{-1}. For the cyclisation step, the CO_3^{2-} anion was again the one to decrease the RIC–TS energy barrier most efficiently (19.16 kcal mol^{-1}), but in this case the second most effective catalyst was Br^- (13.34 kcal mol^{-1}). We must bear in mind, however, that the anions favouring the first step also favoured, in a similar way, the oligomerisation processes competing with the cyclisation. Thus, the overall catalytic effect produced by a given anion was given by comparing the effects calculated for the two steps. The most efficient catalyst for the formation of **7b** should be the one favouring the second step relative to the first one. Thus, calculations showed that Br^- was the most efficient catalyst for the formation of the macrocyclic product: the difference between the decrease in the RIC–TS energy barrier of the second step, relative to the first step, was 8.47 kcal mol^{-1}. The second most efficient anion was CO_3^{2-} with a difference of 6.54 kcal mol^{-1}. All other anions had much less pronounced favourable effects (Cl^-: 4.12 kcal mol^{-1}, AcO^-: 2.26 kcal mol^{-1}, F^-: 1.98 kcal mol^{-1}). The results obtained from the computational calculations were in excellent agreement with experimental observations. We obtained optimal results in the presence of TBABr or K_2CO_3/TBABr, thus confirming the suggested anion kinetic template effect. The computational results also allowed us to justify why F^- gave the worst results, and the fact that the nature of the side chain of the amino acid originally used (phenyl alanine, alanine, valine) insignificantly affected the process. Thus, when the corresponding cyclisations were carried out for the other C_2 open-chain systems (for the formation of macrocycles **7a** and **7c**) using the optimised conditions (CH_3CN, DIPEA, TBABr, at reflux) very similar results were obtained in terms of both yields and kinetics (Figure 12).

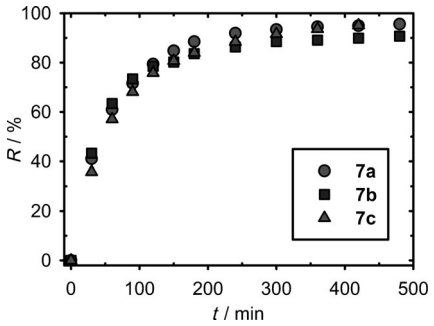

Figure 12. Kinetic curves for the formation of macrocyclic structures **7a–c** in CH_3CN at reflux, using DIPEA as the base and TBABr (0.5 equiv).

A quantitative comparison between the experimental and the computational data can be made through the calculation of the corresponding experimental kinetic parameters. Different kinetic models can be proposed for the complex system outlined in Scheme 2. Some simplifications need to be made to obtain reliable results. We, thus, assumed that the rate constants of the nucleophilic substitutions that gave open-chain compounds were essentially identical ($k_1 = k_p$); this is common for multistep processes.[37,38] This provided a simple kinetic model to which the experimental kinetic data were fit. The kinetic curves obtained with this model reproduced well the main features of the observed curves (Figure 13). In this way, the corresponding kinetic parameters could be calculated (Table 4). Although a perfect quantitative agreement between calculated and experimental parameters was not expected, the calculated kinetic parameters displayed the same trends as those predicted by calculations. Thus, the bromide anion was the most efficient catalyst. Taking into consideration the previous results, we carried out identical calculations for the synthesis of **6**. The ultimate goal of this study was to define the conditions that could allow the preparation of this elusive compound. The simplest side chain ($R = CH_3$) was again selected to facilitate the calculations. The results from the computational calculations revealed some significant patterns (Figures 14, 15, 16,

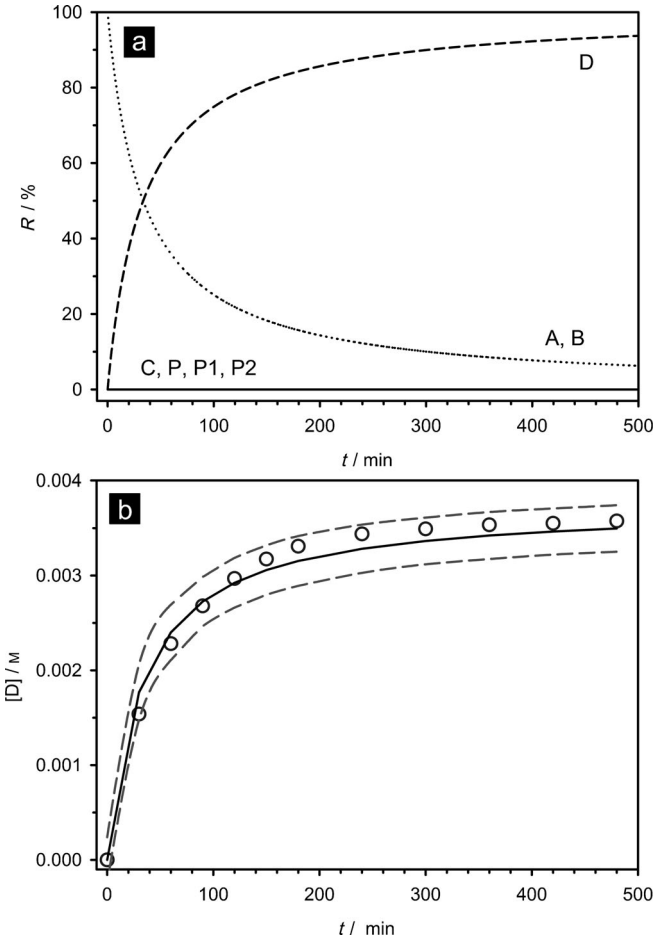

Figure 13. a) Variation of the concentration of the different species (modelled according to the simplified kinetic mode defined in Scheme 2 with $k_1 = k_p$) with time. •••••: [**5a**]; •••••: [1,3-bis(bromomethyl)benzene]; ——: [**8a**]; – – –: [**7a**]. Complete overlap of lines corresponding to the starting materials is observed. The concentration of both the intermediate and the oligomers is very low for the whole time span. b) Variation of the concentration of the macrocyclic compound **7b** (D) with time (under the optimised conditions: DIPEA, TBABr, CH_3CN at reflux); solid line: curve obtained from the calculated k_1 and k_2 values, including standard deviations (– – –); ○: experimental points. A perfect quantitative agreement cannot be expected, but it can be seen how the calculated kinetic parameters display the same trends predicted by calculations.

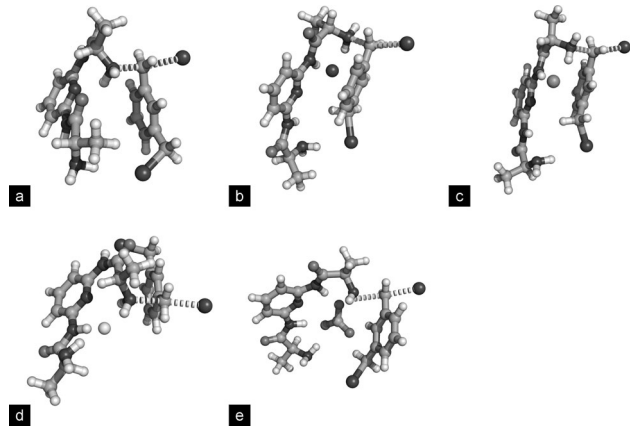

Figure 14. Fully optimised structures (B3LYP/6-31G*) for the TSs for the first reaction step for the preparation of **6b** in the presence of different anions: a) none, b) Br^-, c) Cl^-, d) F^- and e) CO_3^{2-}.

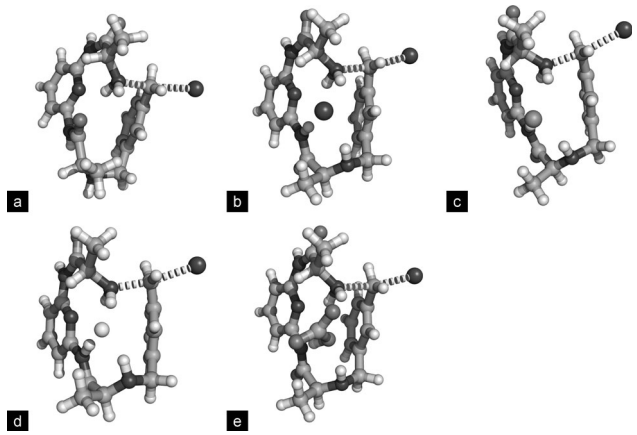

Figure 15. Fully optimised structures (B3LYP/6-31G*) for the TSs for the second reaction for the preparation of **6b** in the presence of different anions: a) none, b) Br^-, c) Cl^-, d) F^- and e) CO_3^{2-}.

and 17, and Tables 5 and 6). As in the case of **7b**, we considered the relative $\Delta\Delta G^{\neq}$ values obtained for both steps in the presence and in the absence of the corresponding anion. The presence of anions resulted in the reduction of the energy barriers, as expected. Nevertheless, the effect of the different anions on the cyclisation step was appreciably smaller than in the case of **7b** (for **7b** $\Delta\Delta G^{\neq}$ values ranged from 11 to 19 kcal mol^{-1}, whereas for **6b** they ranged from 8.8 to 16.1 kcal mol^{-1}). Thus, the stabilisation of the TS through the presence of anions was about 3 kcal mol^{-1} less for **6b** than that for **7b**. In the first step, however, $\Delta\Delta G^{\neq}$ values for **7b** were in the range of 5–12 kcal mol^{-1}, whereas a broader range was calculated for **6b** (3.5–18 kcal mol^{-1}). Overall, the presence of Br^- and Cl^- favoured the

Table 4. Experimental kinetic parameters for the preparation of **7b** under different conditions.

Conditions	k_1 [M^{-1} min^{-1}]	k_2 [min^{-1}]	$\Delta G_1^{\neq}$ [kcal mol^{-1}]	$\Delta G_2^{\neq}$ [kcal mol^{-1}]	$\Delta\Delta G^{\neq}$ [kcal mol^{-1}][a]
K_2CO_3/TBABr[b]	8.0 ± 1.8	33800 ± 100	22.31 ± 0.16	16.42 ± 0.03	−6.21 ± 0.19
DIPEA[b]	2.68 ± 0.20	0.8 ± 0.5	23.08 ± 0.05	23.9 ± 0.4	0.82 ± 0.45
DIPEA/ TBABr[b]	8.0 ± 1.8	33800 ± 100	22.31 ± 0.16	16.42 ± 0.03	−5.89 ± 0.19
DIPEA/ TBACl[b]	2.80 ± 0.17	2.234 ± 0.010	23.05 ± 0.04	23.21 ± 0.10	0.16 ± 0.07
DIPEA/TBAA-cO[b]	3.8 ± 0.6	0.170 ± 0.023	22.84 ± 0.11	25.02 ± 0.10	2.18 ± 0.11
No base, no cat.[b]	2.47 ± 0.17	3091 ± 13	23.13 ± 0.05	18.11 ± 0.03	−5.02 ± 0.08
DIPEA/ TBABr[c]	6.6 ± 1.6	43000 ± 100	22.45 ± 0.16	16.25 ± 0.03	−6.2 ± 1.9
DIPEA/ TBABr[d]	7.9 ± 0.6	5.8 ± 4.4	22.32 ± 0.05	22.5 ± 0.5	0.18 ± 0.55

[a] Calculated as $\Delta G_2^{\neq} - \Delta G_1^{\neq}$. [b] for **7a**. [c] for **7b**. [d] for **7c**.

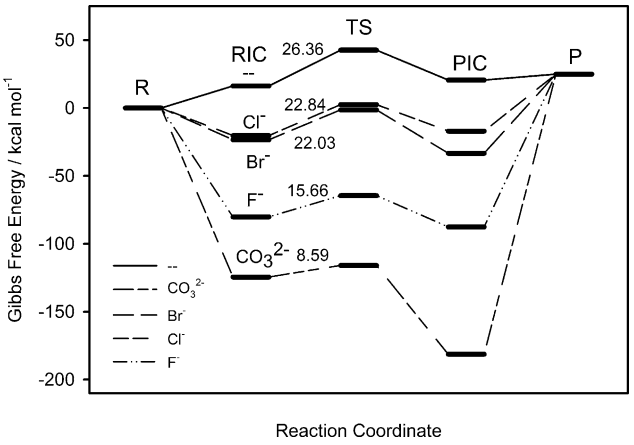

Figure 16. Calculated energy profile for the first step of the reaction in the preparation of **6b** from **4b** and 1,3-bis(bromomethyl)benzene in the presence of different anions. The values for the RIC–TS barrier for each profile have been included [kcal mol^{-1}].

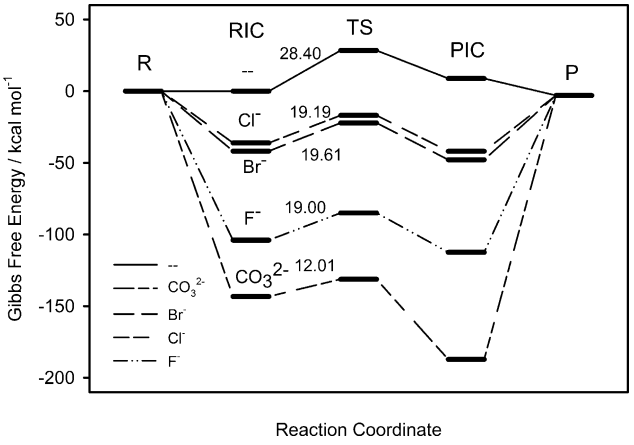

Figure 17. Calculated energy profile for the second step of the reaction in the preparation of **6b** from **4b** and 1,3-bis(bromomethyl)benzene in the presence of different anions. The values for the RIC–TS barrier for each profile have been included [kcal mol^{-1}].

Table 5. Calculated Gibbs energy barriers [kcal mol^{-1}] for the first step of the reaction in the preparation of **6b** from **4b** and 1,3-bis(bromomethyl)benzene in the presence of different anions.

	No cat.	CO_3^{2-}	Br^-	Cl^-	F^-
reactants–RIC	16.26	−124.51	−23.43	−20.38	−80.19
RIC–TS	26.36	8.59	22.03	22.84	15.66
TS–PIC	−22.07	−65.41	−32.02	−19.50	−23.10
PIC–products	4.38	206.26	58.35	41.97	112.57

Table 6. Calculated Gibbs energy barriers [kcal mol^{-1}] for the second step of the reaction in the preparation of **6b** from **4b** and 1,3-bis(bromomethyl)benzene in the presence of different anions.

	No cat.	CO_3^{2-}	Br^-	Cl^-	F^-
reactants–RIC	0.00	−143.27	−41.83	−36.14	−103.97
RIC–TS	28.40	12.01	19.61	19.19	19.00
TS–PIC	−19.60	−55.83	−25.65	−24.96	−27.55
PIC–products	−11.81	184.08	44.86	38.91	109.51

second step over the first one (4.46 and 5.79 kcal mol^{-1}, respectively). On the contrary, the presence of F^- or CO_3^{2-} stabilised the TS of the first step better relative to the cyclisation TS (1.30 and 1.38 kcal mol^{-1}). Except for Cl^-, those values were less favourable for the second step than the ones calculated for the preparation of **7b**. Thus, the computational studies showed that the synthesis of smaller macrocycles (**6**) was less favourable than that of **7**, and this allowed us to rationalise our initial synthetic results. Additionally, it was demonstrated that anions played different roles in each synthetic process. For **6**, we predicted that the smaller Cl^- would have a more pronounced catalytic effect on the macrocyclisation. This was in agreement with the existence of a kinetic template effect in which a specific anionic template was best suited for each specific macrocyclisation process. Based on those results, the use of TBACl/DIPEA in CH_3CN at reflux was expected to give the best results in the synthesis of macrocycles **6**. Accordingly, when the reaction was carried out under those conditions and the precursor **4a** was used, the expected macrocycle **6a** was isolated in 31% yield. Interestingly, in this process the presence of RIC for the cyclisation step was identified in the crude reaction mixture in about 5–10% yields (see the Supporting Information). Compound **6a** was unequivocally identified by HRMS. Nevertheless, the ^{1}H NMR spectra of this compound, taken under different conditions, always showed the presence of complex, relatively broad signals with the expected chemical shifts. More significantly, the ^{13}C NMR spectra also showed the presence of more signals than those expected for a compound such as **6a** (with apparent C_2 symmetry).[39] Even at 60°C the improvement in the signals was very limited (see the Supporting Information). Because the chromatographic data, along with the MS and elemental analyses data revealed the purity of the isolated compound, the ^{1}H NMR spectroscopy results were explained in terms of the existence of several conformers interconverting very slowly on the NMR timescale and/or the existence of a predominant rigid conformer not displaying the expected C_2 symmetry. Conformational analysis of **6b** at the B3LYP/6-31G* level of theory was carried out to get a better understanding of this phenomenon. Calculations revealed the presence of two conformers, separated by 2.49 kcal mol^{-1}, as the most stable ones (Figure 18). Both conformers had a very strained macrocyclic ring. For the most stable conformer, no C_2 symmetry was present, whereas the second con-

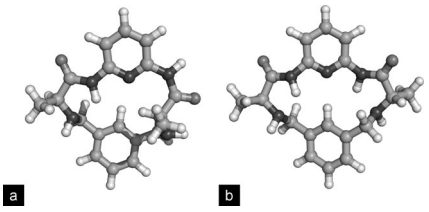

Figure 18. Structures calculated (optimised at the B3LYP/6-31G* level of theory in the gas phase) for the two most stable conformers of **6b**. a) Most stable conformer, non-C_2 symmetric structure; b) second most stable conformer, C_2 symmetric structure.

former displayed such symmetry. Contrary to what was observed in the symmetric conformer, and in most peptidic and pseudopeptidic systems, the most stable conformer contained one strained *cis* amide bond, which seemed to struggle to release some strain.[40] Thus, the presence of the asymmetric structure as the most predominant conformer of **6b**, along with the presence of high interconversion barriers, could explain the complexity of the NMR spectra. The UV-visible and circular dichroism (CD) spectra of compounds **7a–c** and for **6b** were recorded. At the same time, the theoretical CD spectra were calculated computationally for the two fully optimised structures (Figure 18).[41] Solvent effects were taken into account with the use of the polarisable continuum model (PCM) methodology. Excellent agreement between experimental and theoretical CD spectra (corresponding to the minimum energy conformer) was observed (Figure 19). It was evident that the two bands corresponding to **6a** and **7** in the UV spectrum overlapped at about 264 nm and were significantly split at 250 and 297 nm. Most significantly, the CD of **6a** not only displayed a very different pattern (relative to **7**) with a positive signal at 250 nm and a negative one at 297 nm, but also more intense CD effects. This must be due to the higher degree of structural organisation of **6a**.[24]

Conclusion

We clearly demonstrated that the presence of anions significantly affected the course of macrocyclisation reactions in pseudopeptides, peptides and related species, in which supramolecular interactions between the selected anion and the open-chain precursor existed at the TS. The appropriate anionic species acted as a kinetic template that stabilised the TS leading to the macrocyclic structure. Calculations at the B3LYP/6-31G* level of theory enabled rationalisation of those results and showed that the anions considered in this study were able to stabilise the two TSs involved in the formation of **7**: the first one leading to the open-chain intermediate **8** from **5**, and the second one transforming **8** into **7**. The best anionic catalysts were those producing greater stabilisation of the second TS than that of the first one. The effect on the TSs of the competing oligomerisation side reactions and the TS of the transformation of **5** into **8** was similar. In the transformation of **5** to **7**, Br^- was predicted to be the most efficient template and this was in excellent agreement with experimental results. The optimised structures of the corresponding TSs for the macrocyclisation step revealed how the anions acted as efficient templates for this step by facilitating the approach between the two reactive ends on **8**: the anion interacted (electrostatically and through hydrogen bonding) with the two pseudopeptidic fragments. Thus, different anions should be the optimal ones for macrocyclisation reactions involving macrocycles of different sizes. This was evidenced in the preparation of the smaller macrocycle **6a**, the synthesis of which was unsuccessful under standard conditions. Computational calculations revealed that the role of different anions as templates was significantly different. In this case, the smaller Cl^- was best suited to stabilise the TS of the macrocyclisation. Accordingly, the calculations predicted that the best conditions for the synthesis of **6a** involved the use of TBACl, instead of TBABr. This has been experimentally confirmed. Thus, when we used the predicted conditions (TBACl, DIPEA, CH_3CN at reflux) the expected macrocycle **6a** could be isolated in 30% yield. Structural analysis of this smaller macrocycle revealed that the high degree of strain in the structure led to the loss of C_2 symmetry in the minimum-energy conformer and the existence of two different *cis* and *trans* amide bonds.

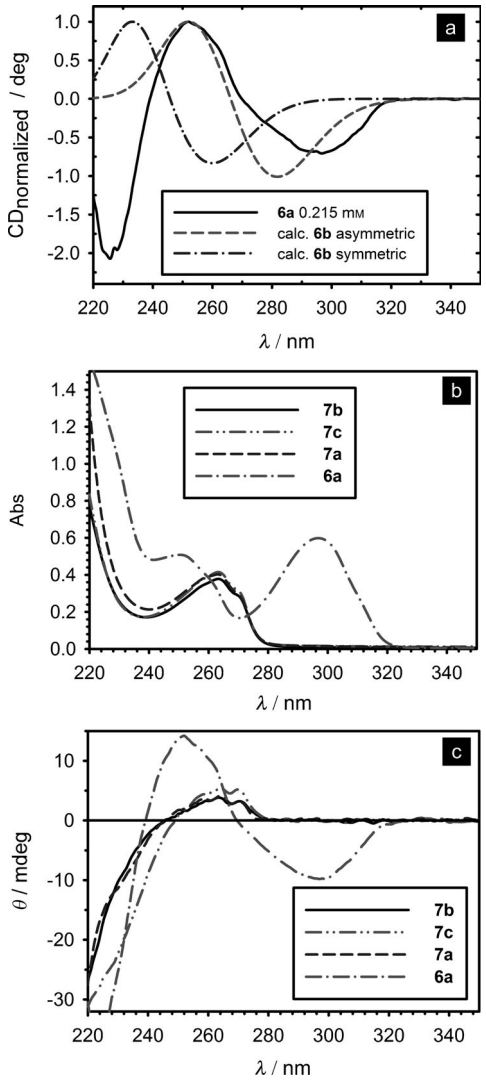

Figure 19. a) Experimental CD spectra for **6a** (——, 0.215 mM in methanol), and calculated CD spectra for the minimum energy conformer (– – –, B3LYP/6-31G* PCM), and the second most stable conformer (–•–•, B3LYP/6-31G* PCM) of **6b**. b) Experimental UV/Vis spectra. c) CD spectra for compounds **7a** (– – –), **7b** (——), **7c** (–••–••) and **6a** (–•–•).

Experimental Section

NMR spectroscopy: NMR spectroscopy experiments were carried out either on a Varian INOVA 500 spectrometer (500 MHz for ^{1}H and 125 MHz for ^{13}C) or a Varian MERCURY 300 spectrometer (300 MHz for ^{1}H and 75 MHz for ^{13}C) at the SCIC (UJI). Chemical shifts are reported in ppm from tetramethylsilane with the solvent resonance as the internal standard. FTIR spectra were recorded by means of a Jasco FT/IR-6200 with an attenuated total reflectance (ATR) adapter. Microanalyses were performed on a CHN Euro EA 3000 elemental analyser. Mass spectra were recorded by means of a Q-TOF Premier (Waters). Rotatory power was determined by means of a Jasco DIP-100 digital polarimeter (Na: 589 nm). Melting points were measured by means of a Melting Points Stuart SMP10 apparatus. CD spectra were recorded on a Jasco J-810 spectropolarimeter. Samples were prepared in a quartz cuvette of 1 cm path length and the measurement temperature was set to 25 °C.

General procedure for the preparation of the pseudopeptides: The starting 2,6-bis(aminomethyl)pyridine was obtained from 2,6-bis(aminomethyl)pyridine hydrochloride (1.000 g, 4.78 mmol) by neutralisation with a 1:1 aqueous solution of NaOH. The resulting aqueous solution was extracted three times with chloroform; the organic phase was dried with anhydrous magnesium sulfate and evaporated in vacuo. The resulting yellowish oil (0.420 g, 3.06 mmol) was dissolved in 1,2-dimethoxyethane (25 mL) in a round-bottomed flask. Cbz-L-Phe-OSu (Cbz = carbobenzyloxy, Su = succinimidyl; 2.427 g, 6.12 mmol, 2 equiv) was dissolved in dimethoxyethane (20 mL) and added to the reaction flask with a pipette. A white precipitate was formed and the mixture was stirred at room temperature for 20 h then heated to 50 °C for 6 h. After cooling, the white precipitate was filtered, washed with cold water (50 mL) and a small amount of methanol then dried under vacuum. The corresponding Cbz-protected open-chain pseudopeptide was obtained as a white solid (90 %, 3.855 g, 5.51 mmol).

Deprotection protocol: The resulting Cbz-protected pseudopeptide (462 mg, 0.66 mmol) was placed in a 100 mL round-bottomed flask. Then, HBr/AcOH (10 mL, 33 %) was added. The resulting yellow solution was stirred under a nitrogen atmosphere for 1 h. The colourless final solution was poured into a 250 mL beaker containing diethyl ether (30 mL). The white precipitate formed was filtered and washed with diethyl ether. The solid was redissolved in distilled water (30 mL). This aqueous phase was washed twice with $CHCl_3$ (10 mL). The aqueous phase was basified with solid NaOH to a pH of 12–13 and then NaCl was added until saturation. The aqueous solution was extracted three times with $CHCl_3$ (25 mL) and the organic phase was dried with anhydrous $MgSO_4$. The solvent was evaporated under reduced pressure and finally dried in an oil vacuum pump to obtain a white solid (88%, 0.249 g, 0.58 mmol).

Compound 5a: M.p. 109–110 °C; $[\alpha]_D^{25} = 69.88$ ($c = 0.01$ in $CHCl_3$); ^{1}H NMR (500 MHz, [D$_6$]DMSO): $\delta = 8.43$ (t, ^3J(H,H) = 5.8 Hz, 2H), 7.57 (t, ^3J(H,H) = 7.7 Hz, 1H), 7.15–7.33 (m, 10H), 6.89 (d, ^3J(H,H) = 7.7 Hz, 2H), 4.31 (ddd, ^3J(H,H) = 5.8, 16.1, 39.9 Hz, 4H), 3.48 (dd, ^3J(H,H) = 5.5, 7.9 Hz, 2H), 2.95 (dd, ^3J(H,H) = 5.4, 13.3 Hz, 2H), 2.67 (dd, ^3J(H,H) = 8.0, 13.3 Hz, 2H), 1.75 ppm (s, 4H); ^{13}C NMR (126 MHz, [D$_6$]DMSO): $\delta = 175.1$, 158.2, 139.2, 137.6, 129.8, 128.6, 126.5, 119.3, 56.9, 44.3, 41.6 ppm; IR (ATR): $\tilde{\nu} = 3363$, 3351, 3293, 3062, 3031, 2916, 2852, 1637, 1591, 1577, 1531, 1494, 1459, 1415 cm^{-1}; HRMS (ESI-TOF): m/z calcd for $C_{25}H_{29}N_5O_2$ $[M+H]^+$: 432.2400; found: 432.2396; elemental analysis calcd (%) for $C_{25}H_{29}N_5O_2$: C 69.58, H 6.77, N 16.23; found: C 69.4, H 6.8, N 16.4.

General procedure for the preparation of 7: Synthesis of 7a: Compound **5a** (605 mg, 1.402 mmol), TBABr (226 mg, 0.701 mmol) and anhydrous K_2CO_3 (1.937 g 14.02 mmol) were placed in a 250 mL round-bottomed flask and then acetonitrile (200 mL) was added to obtain a final concentration of 7 mM for **5a**. The reaction mixture was heated until all of the reactants, except potassium carbonate, were dissolved. Then, 1,3-bis(bromomethyl)benzene (370 mg, 1.402 mmol) was dissolved into a small quantity of dry acetonitrile and added to the reaction flask and the reaction was heated at reflux for 24 h under a nitrogen atmosphere. The reaction mixture was then cooled and filtered by gravity. The filtrate was evaporated under reduced pressure to give the crude product (0.919 g). Purification of the product was carried out by flash column chromatography on silica gel (50 g). CH_2Cl_2/methanol mixtures were used as the mobile phase, containing a few drops of aqueous ammonia to prevent the retention of amines on the column (from 100:0 to 90:3 v/v). The macrocycle **7a** was obtained as a white solid (87 %, 0.525 g, 1.22 mmol). M.p. 70 °C; $[\alpha]_D^{25} = 70.54$ ($c = 0.01$ in $CHCl_3$); ^{1}H NMR (500 MHz, $CDCl_3$): $\delta =$ 1.89 (s, 2H), 2.74–2.90 (m, 2H), 3.27 (dd, ^3J(H,H) = 2.9, 13.8 Hz, 2H), 3.57 (d, ^3J(H,H) = 12.4 Hz, 4H), 3.69 (d, ^3J(H,H) = 12.6 Hz, 2H), 4.38 (d, ^3J(H,H) = 15.2 Hz, 2H), 4.78 (dd, ^3J(H,H) = 6.8, 15.4 Hz, 2H), 6.95 (d, ^3J-(H,H) = 6.6 Hz, 2H), 7.07–7.42 (m, 14H), 7.51–7.75 (m, 2H), 8.36 ppm (s, 2H); ^{13}C NMR (75 MHz, $CDCl_3$): $\delta = 39.1$, 44.5, 53.1, 64.1, 121.6, 127.0, 127.4, 128.1, 128.6, 128.9, 129.3, 137.6, 137.9, 140.0, 156.4, 173.5 ppm; IR (ATR): $\tilde{\nu} = 3359$, 3060, 3027, 2923, 2849, 1658, 1599, 1577, 1497, 1449 cm^{-1}; HRMS (ESI-TOF): m/z calcd for $C_{33}H_{35}N_5O_2$ $[M+H]^+$: 533.2917; found: 533.2917; elemental analysis calcd (%) for $C_{33}H_{35}N_5O_2$: C 74.27, H 6.61, N 13.12; found: C 74.5, H 6.8, N 13.0.

General procedure for the preparation of 4: Synthesis of 4a: Cbz-L-phenylalanine-OH (22.150 g, 74 mmol) and triethylamine (10.3 mL, 74 mmol) were dissolved in dry THF (400 mL). The solution was cooled to −5 °C and then ethylchloroformiate (7.3 mL, 74 mmol) was added to the reaction flask and it was stirred for 30 min at −5 °C under a nitrogen atmosphere. 2,6-Diaminopyridine (22.150 g, 74 mmol) was dissolved in dry THF (25 mL) and added dropwise to the reaction flask in 15 min. The reaction was stirred for 1 h at −5 °C under a nitrogen atmosphere. After this period, the reaction was filtered and the solvent was evaporated under reduced pressure. The resulting foam was dissolved in ethyl acetate (200 mL) and washed with water (3 × 50 mL), a saturated aqueous solution of $NaHCO_3$ (3 × 50 mL) and a saturated aqueous solution of NaCl (3 × 50 mL). The organic phase was dried with $MgSO_4$ and the solvent was evaporated under reduced pressure. The crude product was purified by flash chromatography column on silica gel with hexane/ethyl acetate (7:3) as the eluent. The product (**4a**) was obtained as a white foam (57 %, 14.050 g, 20.9 mmol). M.p. 109–110 °C; $[\alpha]_D^{25} = 50.5$ ($c = 0.01$ in DMSO); ^{1}H NMR (500 MHz, CD_3CN): $\delta = 9.64$ (s, 2H), 7.92 (d, ^3J-(H,H) = 8.0 Hz, 2H), 7.78 (t, ^3J(H,H) = 8.0 Hz, 1H), 7.44–7.11 (m, 10H), 3.69 (dd, ^3J(H,H) = 4.4, 8.6 Hz, 2H), 3.21 (dd, ^3J(H,H) = 4.4, 13.8 Hz, 2H), 2.83 (dd, ^3J(H,H) = 8.7, 13.7 Hz, 2H), 1.74 ppm (s, 4H); ^{13}C NMR (75 MHz, [D$_6$]DMSO): $\delta = 174.6$, 150.5, 141.2, 139.1, 130.0, 128.8, 126.9, 108.8, 57.3, 41.1 ppm; IR (ATR): $\tilde{\nu} = 3292$, 1637, 1533 cm^{-1}; HRMS (ESI-TOF): m/z calcd for $C_{25}H_{29}N_5O_2$ $[M+H]^+$: 404.2087; found: 404.2091; elemental analysis calcd (%) for $C_{25}H_{29}N_5O_2$: C 69.58, H 6.77, N 16.23; found: C 69.4, H 6.7, N 16.1.

General procedure for the preparation of 6: Synthesis of 6a: Compound **4a** (1.000 g, 2.478 mmol), TBACl (344 mg, 1.239 mmol) and DIPEA (4.24 mL, 24.78 mmol) were placed in a round-bottomed flask and then dry acetonitrile (600 mL) was added. The reaction mixture was heated until all of the reactants were dissolved. Then, 1,3-bis(bromomethyl)benzene (654 mg, 2.478 mmol) was dissolved in a small quantity of dry acetonitrile and placed into the reaction flask and the reaction was heated at reflux for 24 h under a nitrogen atmosphere. The reaction mixture was then cooled and the solvent was evaporated under reduced pressure to give the crude product as a foam. Purification of this product was carried out by flash column chromatography on flash silica gel. CH_2Cl_2/methanol mixtures were used as the mobile phase, containing a few drops of aqueous ammonia to prevent the retention of amines on the column (from 450:6 to 480:8 v/v). The macrocycle (**6a**) was obtained as a white solid (31 %, 393 mg, 0.777 mmol). M.p. 95 °C; $[\alpha]_D^{25} = -128.18$ ($c = 0.01$ in $CHCl_3$); ^{1}H NMR (500 MHz, $CDCl_3$) $\delta = 9.97$–9.01 (m, 2H), 7.98 (m, 1H), 7.65 (m, 2H), 7.32—6.92 (m, 15H), 3.92—2.97 (m, 8H), 2.80 (m, 2H), 2.07 ppm (s, 3H); ^{13}C NMR (125 MHz, $CDCl_3$) $\delta = 172.9$, 172.5, 172.4, 149.4, 149.1, 140.63, 140.57, 139.1, 139.0, 137.6, 137.0, 129.3, 129.1, 129.0, 128.8, 128.7, 127.7, 127.6, 127.1, 127.04, 126.97, 126.3, 109.5, 109.4, 107.8, 63.4, 56.9, 52.3, 40.6, 39.12, 39.07 ppm; IR (ATR): $\tilde{\nu} = 3085$, 3025, 2844, 1676, 1582, 1516, 1493, 1442, 1391, 1292, 1241 cm^{-1}; HRMS (ESI-TOF): m/z calcd for $C_{31}H_{31}N_5O_2$ $[M+H]^+$: 506.2556; found: 506.2550; elemental analysis calcd (%) for $C_{31}H_{31}N_5O_2$ H_2O: C 71.11, H 6.35, N 13.37; found: C 70.9, H 6.5, N 13.5.

Kinetic analysis of the cyclisation of 7 by HPLC: Experiments under different reaction conditions were carried out. In all cases, the solvent was acetonitrile. Thus, for instance, bis-amidoamine **7a** (49.3 mg, 0.187 mmol), DIPEA (320 μL, 1.870 mmol), TBABr (30.1 mg, 0.093 mmol) and mesitylene (25 μL), as the internal standard, were placed in a round-bottomed flask equipped with a magnetic stirrer and a condenser under a nitrogen atmosphere. Then, dry acetonitrile (50.00 mL) was added and the system was heated to 81.6 °C. Afterwards, 1,3-bis(bromomethyl)benzene (49.3 mg, 0.187 mmol) was added to the reaction mixture and this was assumed as the initial point of the reaction. Aliquots were initially taken every 30 min and then every 1 h for a total of 8 h. The aliquots were not further diluted. When K_2CO_3 was used as the base, it was removed by filtration by means of a HPLC syringe filter. The HPLC vials were rapidly cooled in an ice bath and the chromatogram was recorded immediately. The HPLC was equipped with a Protonsil 120-5-C18 column with the detector adjusted at 210 nm. The volume of injection was 0.5 μL. The mobile phase was acetonitrile/H_2O (80:20) and the flow was 1 mL min^{-1}. The temperature was set at 35 °C and the chromatogram was registered for 15 min.

Kinetic analysis of the cyclisation of 7a by ^{1}H NMR spectroscopy: In this experiment tetrakis(trimethylsilyl)silane (0.056 equiv) was used as the internal standard. This allowed us to quantify the signals of the product and the starting reactants. We performed the experiments directly in an NMR tube at different temperatures, depending on the experiment (from 25 °C to 50 °C), using CD_3CN (1.00 mL). The concentration of the starting material was 7.5 mM. For this purpose, the bis-amidoamine catalyst, base and internal standard were placed in a vial. Then CD_3CN was added and the reaction mixture was stirred and heated until a clear solution was obtained. The reaction mixture was transferred quantitatively to an NMR tube. Then, the initial NMR spectrum was acquired. Then the contents of the NMR tube were quantitatively transferred to a vial containing 1,3-bis(bromomethyl)benzene, mixed and immediately transferred back to the NMR tube. An NMR spectrum was acquired every 15 min at least for 12 h.

Computational calculations: All structures where minimised by using the Gaussian 03 program. All of the calculations were performed in the gas phase. The nature of the minima was demonstrated by a normal mode of vibration analysis. For TSs, one single negative eigenvalue was found, corresponding to the reaction path involving the breaking and forming of bonds. For the other structures all of the eigenvalues were positive.

Acknowledgements

This work was supported by the Spanish Ministry of Science and Innovation (CTQ2009-14366-C02) and UJI-Bancaixa (P1-1B-2009-59). V.M-C. thanks the MICINN for personal financial support (FPU fellowship). The support of the SCIC of the UJI for the different instrumental techniques is acknowledged.

[1] a) *Modern Supramolecular Chemistry: Strategies for Macrocycle Synthesis* (Eds.: F. Diederich, P. Stang, R. R. Tykwinski), Wiley-VCH, Weinheim, **2008**; b) *Macrocycle Synthesis: A Practical Approach*, (Ed.: D. Parker), Oxford University Press, Oxford, **1996**.

[2] a) A. Yonath, *Angew. Chem.* **2010**, *122*, 4438–4453; *Angew. Chem. Int. Ed.* **2010**, *49*, 4340–4354; b) A. Yonath, *Annu. Rev. Biochem.* **2005**, *74*, 649–679; c) T. Auerbach, I. Mermershtain, C. Davidovich, A. Bashan, M. Belousoff, I. Wekselman, E. Zimmerman, L. Q. Xiong, D. Klepacki, K. Arakawa, H. Kinashi, A. S. Mankin, A. Yonath, *Proc. Natl. Acad. Sci. USA* **2010**, *107*, 1983–1988.

[3] a) J. D. Craik, *Science* **2006**, *311*, 1563–1564; b) J. Rizo, L. M. Gierasch, *Annu. Rev. Biochem.* **1992**, *61*, 387–418; c) R. Kenien, *Accessibility of a Cyclopeptide Towards Thrombin-Catalyzed Proteolysis*, VDM Verlag Dr. Müller, Saarbrücken (Germany), **2010**.

[4] a) C. R. Moellering, *Clin. Infect. Dis.* **2006**, *42*, S3-S4; b) D. P. Levine, *Clin. Infect. Dis.* **2006**, *42*, S5-S12 and references therein.

[5] a) H. J. Lee, A. H. Macbeth, J. Pagani, W. S. Young, *Prog. Neurobiol.* **2009**, *88*, 127–151; b) *Vasopressin And Oxytocin: From Genes To Clinical Applications*, Prog. Brain Res. 139, (Eds: D. Poulain, S. Oliet, D. Theodosis), Elsevier, Amsterdam, **2002**.

[6] S. L. Schreiber, G. R. Crabtree, *Immunol. Today* **1992**, *13*, 136–142.

[7] R. M. Kohli, C. T. Walsh, M. D. Burkart, *Nature* **2002**, *418*, 658–660.

[8] a) K. Umezawa, Y. Ikeda, Y. Uchihata, H. Nayanawa, S. Kondo, *J. Org. Chem.* **2000**, *65*, 459–463; b) see also: S. M. Yu, W. X. Hong, Y. Wu, C. L. Zhong, Z. J. Yao, *Org. Lett.* **2010**, *12*, 1124–1127.

[9] a) T. Rezai, B. Yu, G. L. Millhauser, M. P. Jacobson, R. S. Lokey, *J. Am. Chem. Soc.* **2006**, *128*, 2510–2511; b) A. Geyer, G. Müller, H. Kessler, *J. Am. Chem. Soc.* **1994**, *116*, 7735–7743; c) F. Al-Obeidi, A. M. Castrucci, M. E. Hadley, V. J. Hruby, *J. Med. Chem.* **1989**, *32*, 2555–2561.

[10] D. Besser, B. Muller, P. Kleinwachter, G. Greiner, L. Seyfarth, T. Steinmetzer, O. Arad, S. Reissmann, *J. Prakt. Chem.* **2000**, *342*, 537–545.

[11] a) K. Gloe, *Macrocyclic Chemistry: Current Trends and Future Perspectives*, Springer, Dordrecht, **2005**; b) D. Parker, *Macrocycle Synthesis: A Practical Approach*, Oxford University Press, New York, **1996**; c) B. Dietrich, P. Viout, J. M. Lehn, *Macrocyclic Chemistry*, VCH, Weinheim, **1993**; d) F. Vögtle, *Cyclophane Chemistry*, Wiley, Chichester, **1993**; e) N. Sokolenko, G. Abbenante, M. J. Scanlon, A. Jones, L. R. Gahan, G. R. Hanson, D. P. Fairlie, *J. Am. Chem. Soc.* **1999**, *121*, 2603–2604.

[12] For an analysis of thermodynamically controlled macrocyclisations, see: M. M. C. Bastings, T. F. A. de Greef, J. L. J. van Dongen, M. Merkx, E. W. Meijer, *Chem. Sci.* **2010**, *1*, 79–88, and references therein.

[13] For an analysis of kinetically controlled macrocyclisations, see: a) W. Feng, K. Yamato, L. Yang, J. S. Ferguson, L. Zhong, S. Zou, L. Yuan, X. C. Zeng, B. Gong, *J. Am. Chem. Soc.* **2009**, *131*, 2629–2637; b) J. S. Ferguson, K. Yamato, R. Liu, H. Lan, X. C. Zeng, B. Gong, *Angew. Chem.* **2009**, *17*, 3196–3200; *Angew. Chem. Int. Ed.* **2009**, *48*, 3150–3154; c) X. Zhao, Z. T. Li, *Chem. Commun.* **2010**, *46*, 1601–1616.

[14] a) L. G. Nair, S. Bogen, F. Bennett, K. Chen, B. Vibulbhan, Y. Huang, W. Yang, R. J. Doll, N. Y. Shih, G. F. Njoroge, *Tetrahedron Lett.* **2010**, *51* 3057–3061; b) F. Bernal, A. F. Tyler, S. J. Korsmeyer, L. D. Walensky, G. L. Verdine, *J. Am. Chem. Soc.* **2007**, *129*, 2456–2457; c) C. Hebach, U. Kazmaier, *Chem. Commun.* **2003**, 596–597; d) H. E. Blackwell, J. D. Sadowsky, R. J. Howard, J. N. Sampson, J. A. Chao, W. E. Steinmetz, D. J. O'Leary, R. H. Grubbs, *J. Org. Chem.* **2001**, *66*, 5291–5302.

[15] O. E. Vercillo, C. K. Z. Andrade, L. A. Wessjohann, *Org. Lett.* **2008**, *10*, 205–208.

[16] a) A. A. Aimetti, R. K. Shoemaker, C. C. Linc, K. S. Anseth, *Chem. Commun.* **2010**, *46*, 4061–4063; b) R. A. Turner, A. G. Oliver, R. S. Lokey, *Org. Lett.* **2007**, *9*, 5011–5014; c) V. D. Bock, R. Perciaccante, T. P. Jansen, H. Hiemstra, J. H. van Maarseveen, *Org. Lett.* **2006**, *8*, 919–922; d) S. Punna, J. Kuzelka, Q. Wang, M. G. Finn, *Angew. Chem.* **2005**, *117*, 2255–2260; *Angew. Chem. Int. Ed.* **2005**, *44*, 2215–2220.

[17] a) J. A. McIntosh, R. C. Robertson, V. Agarwal, S. K. Nair, G. W. Bulaj, E. W. Schmidt, *J. Am. Chem. Soc.* **2010**, *132*, 15499–15501; b) F. Kopp, M. A. Marahiel, *Nat. Prod. Rep.* **2007**, *24*, 735–749; c) D. Schwarzer, R. Finking, M. A. Marahiel, *Nat. Prod. Rep.* **2003**, *20*, 275–287.

[18] a) H. Shimamura, S. P. Breazzano, J. Garfunkle, F. S. Kimball, J. D. Trzupek, D. L. Boger, *J. Am. Chem. Soc.* **2010**, *132*, 7776–7783; b) B. Yoo, S. B. Y. Shin, M. L. Huang, K. Kirshenbaum, *Chem. Eur. J.* **2010**, *16*, 5528–5537; c) Y. Ding, W. H. Seufert, Z. Q. Beck, D. H. Sherman, *J. Am. Chem. Soc.* **2008**, *130*, 5492–5498; d) Y. Hamada, T. Shioiri, *Chem. Rev.* **2005**, *105*, 4441–4482; e) T. Shioiri, Y. Hamada, *Synlett* **2001**, 184–201; f) J. N. Lambert, J. P. Mitchell, K. D. Roberts, *J. Chem. Soc. Perkin Trans. 1* **2001**, 471–484; g) A. B. Tabor, *The Chemical Synthesis of Natural Products*; (Ed: K. J. Hale), Academic Press Ltd., Sheffield, **2000**, Chapter 11; h) K. J. Hale, G. S. Bhatia, M. Frigerio, *The Chemical Synthesis of Natural*

Products, (Ed: K. J. Hale), Academic Press Ltd., Sheffield, **2000**, Chapter 12; i) P. Wipf, *Chem. Rev.* **1995**, *95*, 2115–2134; j) J. M. Humphrey, A. R. Chamberlin, *Chem. Rev.* **1997**, *97*, 2243–2266; k) J. P. Tam, Y. A. Lu, Q. Yu, *J. Am. Chem. Soc.* **1999**, *121*, 4316–4324.

[19] a) S. B. Y. Shin, B. Yoo, L. J. Todaro, K. Kirshenbaum, *J. Am. Chem. Soc.* **2007**, *129*, 3218–3225; b) D. G. Rivera, L. A. Wessjohann, *J. Am. Chem. Soc.* **2006**, *128*, 7122–7123; c) H. Jiang, J. M. Léger, P. Guionneau, I. Huc, *Org. Lett.* **2004**, *6*, 2985–2988; d) T. Velasco-Torrijos, P. V. Murphy, *Org. Lett.* **2004**, *6*, 3961–3964; e) M. Amorín, L. Castedo, J. R. Granja, *Chem. Eur. J.* **2008**, *14*, 2100–2111; f) Interesting examples of this concept can also be found in the field of oligosaccharides: M. L. Gening, D. V. Titov, A. A. Grachev, A. G. Gerbst, O. N. Yudina, A. S. Shashkov, A. O. Chizhov, Y. E. Tsvetkov, N. E. Nifantiev, *Eur. J. Org. Chem.* **2010**, 2465–2475.

[20] a) R. Hili, V. Rai, A. K. Yudin, *J. Am. Chem. Soc.* **2010**, *132*, 2889–2891; b) S. Colombo, C. Coluccini, M. Caricato, C. Gargiulli, G. Gattuso, D. Pasini, *Tetrahedron* **2010**, *66*, 4206–4211.

[21] a) J. Becerril, M. Bolte, M. I. Burguete, F. Galindo, E. García-España, S. V. Luis, J. Miravet, *J. Am. Chem. Soc.* **2003**, *125*, 6677–6686; b) M. I. Burguete, B. Escuder, E. García-España, L. López, S. V. Luis, J. Miravet, M. Querol, *Tetrahedron Lett.* **2002**, *43*, 1817–1819.

[22] a) I. Alfonso, M. Bolte, M. Bru, M. I. Burguete, S. V. Luis, *Chem. Eur. J.* **2008**, *14*, 8879–8891; b) M. Bru, I. Alfonso, M. I. Burguete, S. V. Luis, *Tetrahedron Lett.* **2005**, *46*, 7781–7785.

[23] Interesting match/mistmach effects have also been observed in the macrocyclisation of some linear peptides enabled by amphoteric molecules, see: J. Rubio, I. Alfonso, M. Bru, M. I. Burguete, S. V. Luis, *Tetrahedron Lett.* **2010**, *51*, 5861–5867.

[24] a) I. Alfonso, M. Bolte, M. Bru, M. I. Burguete, S. V. Luis, J. Rubio, *J. Am. Chem. Soc.* **2008**, *130*, 6137–6144; b) M. Bru, I. Alfonso, M. I. Burguete, S. V. Luis, *Angew. Chem.* **2006**, *118*, 6301–6305; *Angew. Chem. Int. Ed.* **2006**, *45*, 6155–6159.

[25] a) *Template Synthesis of Macrocyclic Compounds*, (Eds.: N. V. Gerbeleu, V. B. Arion, J. Burgess), Wiley-VCH, Weinheim, **1999**; b) D. H. Busch, A. L. Vance, G. Kolchinski, in *Comprehensive Supramolecular Chemistry, Vol. 9* (Ed: J. M. Lehn), Elsevier, New York, **1996**, pp. 1–42; c) *Comprehensive Supramolecular Chemistry, Vol. 11*. (Eds.: J. L. Atwood, J. E. D. Davies, D. D. MacNicol, F. Vogtle), Pergamon, Oxford, **1996**.

[26] a) B. Lewandowski, S. Jarosz, *Org. Lett.* **2010**, *12*, 2532–2535; b) N. Gimeno, R. Vilar, *Coord. Chem. Rev.* **2006**, *250*, 3161–3189; c) R. Vilar, *Angew. Chem.* **2003**, *115*, 1498–1516; *Angew. Chem. Int. Ed.* **2003**, *42*, 1460–1477.

[27] a) M. I. Burguete, F. Galindo, R. Gavara, M. Izquierdo, J. Lima, S. V. Luis, A. Parola, F. Pina, *Langmuir*, **2008**, *24*, 9795–9803; b) F. Galindo, M. I. Burguete, M.; R. Gavara, S. V. Luis, *J. Photochem. Photobiol. A* **2006**, *178*, 57–61; R. Gavara, S. V. Luis, *J. Photochem. Photobiol. A* **2006**, *178*, 57–61; c) J. Becerril, B. Escuder, J. Miravet, R. Gavara, S. V. Luis, *Eur. J. Org. Chem.* **2005**, 481–485; d) J. Becerril, M. I. Burguete, B. Escuder, F. Galindo, R. Gavara, J. Miravet, S. V. Luis, G. Peris, *Chem. Eur. J.* **2004**, *10*, 3879–3890.

[28] a) J. Becerril, M. Bolte, M. I. Burguete, J. Escorihuela, F. Galindo, S. V. Luis, *Cryst. Eng. Comm.* **2010**, *12*, 1722–1725; b) I. Alfonso, M. Bolte, M. Bru, M. I. Burguete, S. V. Luis, *Cryst. Eng. Comm.* **2009**, *11*, 735–738; c) S. Blasco, M. I. Burguete, M. P. Clares, E. García-España, J. Escorihuela, S. V. Luis, *Inorg. Chem.* **2010**, *49*, 7841–7852; d) I. Alfonso, M. Bolte, M. Bru, M. I. Burguete, S. V. Luis, *Chem. Eur. J.* **2008**, *14*, 8879–8891.

[29] a) I. Alfonso, M. Bru, M. I. Burguete, E. García-Verdugo, S. V. Luis, *Chem. Eur. J.* **2010**, *16*, 1246–55; b) J. Becerril, M. I. Burguete, B. Escuder, S. V. Luis, J. F. Miravet, M. Querol, *Chem. Commun.* **2002**, 738–739.

[30] a) R. Polt, B. D. Kelly, B. D. Dangel, U. B. Tadikonda, R. E. Ross, A. M. Raitsimring, A. V. Astashkin, *Inorg. Chem.* **2003**, *42*, 566–574; b) B. Dangel, M. Clarke, J. Haley, D. Sames, R. Polt, *J. Am. Chem. Soc.* **1997**, *119*, 10865–10866.

[31] a) Ph. D. Dissertation Jorge Escorihuela, Univ. Jaume I Castellón **2009**; b) J. Escorihuela, M. I. Burguete, S. V. Luis, *Tetrahedron Lett.* **2008**, *49*, 6885–6888; c) M. I. Burguete, M. Collado, J. Escorihuela, F. Galindo, E. García-Verdugo, S. V. Luis, M. Vicent, *Tetrahedron Lett.* **2003**, *44*, 6891–6894.

[32] a) I. Alfonso, M. I. Burguete, S. V. Luis, J. F. Miravet, P. Seliger, E. Tomal, *Org. Biomol. Chem.* **2006**, *4*, 853–859; b) R. H. Yang, W. H. Chan, A. W. M. Lee, P. F. Xia, H. K. Zhang, *J. Am. Chem. Soc.* **2003**, *125*, 2884–2885.

[33] a) J. Alarcón, M. T. Albelda, R. Belda, M. P. Clares, E. Delgado-Pinar, J. C. Frías, E. García-España, J. González, C. Soriano, *Dalton Trans.* **2008**, 6530–6538; b) A. González-Álvarez, I. Alfonso, P. Díaz, E. García-España, V. Gotor-Fernández, V. Gotor, *J. Org. Chem.* **2008**, *73*, 374–382; c) B. Verdejo, S. Blasco, E. García-España, F. Lloret, *Dalton Trans.* **2007**, 4726–4737; d) A. Bencini, A. Bianchi, A. Danesi, C. Giorgi, P. Mariani, *J. Coord. Chem.* **2009**, *62*, 82–91; e) A. Bencini, A. Bianchi, S. Del Piero, C. Giorgi, A. Melchior, R. Portanova, M. Tolazzi, B. Valtancoli, *J. Solution Chem.* **2008**, *37*, 503–517.

[34] a) M. J. Alcón, M. Iglesias, F. Sánchez, I. Viani, *J. Organomet. Chem.* **2000**, *601*, 284–292.

[35] a) Gaussian 03, Revision B.04, M. J. Frisch, G. W. Trucks, H. B. Schlegel, G. E. Scuseria, M. A. Robb, J. R. Cheeseman, J. A. Montgomery, Jr., T. Vreven, K. N. Kudin, J. C. Burant, J. M. Millam, S. S. Iyengar, J. Tomasi, V. Barone, B. Mennucci, M. Cossi, G. Scalmani, N. Rega, G. A. Petersson, H. Nakatsuji, M. Hada, M. Ehara, K. Toyota, R. Fukuda, J. Hasegawa, M. Ishida, T. Nakajima, Y. Honda, O. Kitao, H. Nakai, M. Klene, X. Li, J. E. Knox, H. P. Hratchian, J. B. Cross, V. Bakken, C. Adamo, J. Jaramillo, R. Gomperts, R. E. Stratmann, O. Yazyev, A. J. Austin, R. Cammi, C. Pomelli, J. W. Ochterski, P. Y. Ayala, K. Morokuma, G. A. Voth, P. Salvador, J. J. Dannenberg, V. G. Zakrzewski, S. Dapprich, A. D. Daniels, M. C. Strain, O. Farkas, D. K. Malick, A. D. Rabuck, K. Raghavachari, J. B. Foresman, J. V. Ortiz, Q. Cui, A. G. Baboul, S. Clifford, J. Cioslowski, B. B. Stefanov, G. Liu, A. Liashenko, P. Piskorz, I. Komaromi, R. L. Martin, D. J. Fox, T. Keith, M. A. Al-Laham, C. Y. Peng, A. Nanayakkara, M. Challacombe, P. M. W. Gill, B. Johnson, W. Chen, M. W. Wong, C. Gonzalez, and J. A. Pople, Gaussian, Inc., Wallingford CT, **2004**; b) H. Eyring, *J. Chem. Phys.* **1935**, *3*, 107–115; c) K. Fukui, *Acc. Chem. Res.* **1981**, *12*, 363–368; d) C. Lee, W. Yang, R. G. Parr, *J. Chem. Phys.* **1972**, *56*, 2257–2261; e) A. D. Becke, *J. Chem. Phys.* **1993**, *98*, 5648–5652; f) K. J. Laidler, M. C. Klng, *J. Phys. Chem.* **1983**, *87*, 2657–2664; g) D. G. Truhlar, W. L. Hase, J. T. Hynes, *J. Phys. Chem.* **1983**, *87*, 2664–2682; h) D. G. Truhlar, B. C. Garrett, S. J. Klippenstein, *J. Phys. Chem.* **1996**, *100*, 12771–12800; i) A. G. Algarra, M. G. Basallote, M. Feliz, M. J. Fernández-Trujillo, R. Llusar, V. S. Safont, *Chem. Eur. J.* **2006**, *12*, 1413–1426.

[36] Many examples can be found in the literature on the importance of supramolecular interactions at the TS. This is illustrated by the study of reactions in which the reactants are encapsulated in molecular containers: J. Rebek, *Acc. Chem. Res.* **2009**, *42*, 1660–1668.

[37] a) I. C. Sanchez, *Ind. Eng. Chem. Res.* **2010**, *49*, 11890–11895; b) R. M. Ziff, *J. Stat. Phys.* **1980**, *23*, 241–263; c) D. Yan, *Macromolecules* **1998**, *31*, 563–572; d) M. Szwark, *Nature* **1956**, *178*, 1168–1169; e) P. J. Flory, *J. Am. Chem. Soc.* **1940**, *62*, 1561–1565; f) P. J. Flory, *J. Am. Chem. Soc.* **1939**, *61*, 3334–3340; g) P. J. Flory, *J. Am. Chem. Soc.* **1940**, *62*, 255–2261; h) C. W. Bielawski, D. Benitez, R. H. Grubbs, *Science* **2010**, 2041–2044; i) K. Ishizu, *Polymer* **1996**, *37*, 1487–1492; j) D. E. Lonsdale, C. A. Bell, M. J. Monteiro, *Macromolecules* **2010**, *43*, 3331–3339; k) Y. Yu, G. Storti, M. Morbidelli, *Macromolecules* **2009**, *42*, 8187–8197; l) A. Takano, Y. Kushida, K. Aoki, K. Masuoka, K. Hayashida, D. Cho, D. Kawaguchi, Y. Matsushita, *Macromolecules* **2007**, *40*, 679–681; m) M. A. Winnik, T. Redpath, D. H. Richards, *Macromolecules* **1980**, *13*, 328–335; n) H. R. Kricheldorf, M. Al-Masri, G. Schwarz, *Macromolecules* **2002**, *35*, 8936–8942; o) D. E. Lonsdale, M. J. Monteiro, *J. Polym. Sci. Part A* **2010**, *48*, 4496–4503; p) H. R. Kricheldorf, *Polymer* **2010**, *48*, 251–284; q) E. S. Espinoza, W. E. V. Narváez, *J. Mass Spectrom.*

2010, *45*, 722–33; r) B. Laurent, S. M. Grayson, *Chem. Soc. Rev.* **2009**, *38*, 2202–13; s) S. H. Kyne, C. Y. Lin, I. Ryu, M. L. Coote, C. H. Schiesser, *Chem. Commun.* **2010**, *46*, 6521–6523; t) M. Winnik, *Acc. Chem. Res.* **1985**, *18*, 73–79.

[38] a) K. Yu, W. Sommer, J. M. Richardson, M. Weck, C. W. Jones, *Adv. Synth. Catal.* **2005**, *347*, 161–171; b) M. A. Watzky, R. G. Finke, *J. Am. Chem. Soc.* **1997**, *119*, 10382–10400; c) K. S. Weddle, J. D. Aiken III, R. G. Finke, *J. Am. Chem. Soc.* **1998**, *120*, 5653–5666; d) J. A. Widegren, J. D. Aiken III, S. Azkar, R. G. Finke, *Chem. Mater.* **2001**, *13*, 312–324; e) J. A. Widegren, M. A. Bennett, R. G. Finke, *J. Am. Chem. Soc.* **2003**, *125*, 10301–10310; f) J. A. Widegren, R. G. Finke, *J. Mol. Catal. A* **2003**, *198*, 317–341.

[39] a) M. Bru, I. Alfonso, M. Bolte, M. I. Burguete, S. V. Luis, *Chem. Commun.* **2011**, *47*, 283–285; b) I. Alfonso, M. I. Burguete, F. Galindo, S. V. Luis, L. Vigara, *J. Org. Chem.* **2007**, *72*, 7947–7956; c) I. Alfonso, M. I. Burguete, S. V. Luis, *J. Org. Chem.* **2006**, *71*, 2242–2250.

[40] a) K. Nguyen, M. Iskandar, D. L. Rabenstein, *J. Phys. Chem. B* **2010**, *114*, 3387–3392; b) M. Hosoya, Y. Otani, M. Kawahata, K. Yamaguchi, T. Ohwada, *J. Am. Chem. Soc.* **2010**, *132*, 14780–14789; c) G. Revilla-López, A. I. Jiménez, C. Cativiela, R. Nussinov, C. Alemán, D. Zanuy, *J. Chim. Infor. Model.* **2010**, *50*, 1781–1789.

[41] a) N. Berova, L. Di Bari, G. Pescitelli, *Chem. Soc. Rev.* **2007**, *36*, 914–931; b) J. L. Alonso-Gómez, P. Rivera-Fuentes, N. Harada, N. Berova, F. Diederich, *Angew. Chem.* **2009**, *121*, 5653–5656; *Angew. Chem. Int. Ed.* **2009**, *48*, 5545–5548; c) E. Giorgio, K. Tanaka, W. Ding, G. Krishnamurthy, K. Pitts, G. A. Ellestad, C. Rosini, N. Berova, *Bioorg. Med. Chem.* **2005**, *13*, 5072–5079; d) E. Giorgio, K. Tanaka, L. Verotta, K. Nakanishi, N. Berova, C. Rosini, *Chirality* **2007**, *445*, 434–445.

Received: May 9, 2011
Revised: September 20, 2011
Published online: January 19, 2012

